Monograph:
Guo, L.Z., Mei, S.S. and Billings, S.A. (2002) Neighbourhood Detection and Identification of Spatio-Temporal Dynamical Systems Using a Course-To-Fine Approach. Research Report. ACSE Research Report 828 . Department of Automatic Control and Systems Engineering

NEIGHBOURHOOD DETECTION AND IDENTIFICATION OF SPATIO-TEMPORAL DYNAMICAL SYSTEMS USING A COARSE-TO-FINE APPROACH

L.Z. GUO, S.S. MEI AND S.A.BILLINGS

Department of Automatic Control and Systems Engineering
University of Sheffield
Sheffield, S1 3JD
UK

Research Report No. 828
November 2002

Neighbourhood Detection and Identification of Spatio-Temporal Dynamical Systems Using a Coarse-to-Fine Approach

L.Z.Guo, S.S.Mei and S.A. Billings

Department of Automatic Control and Systems Engineering
University of Sheffield
Sheffield S1 3JD, UK

Abstract

A novel approach to the determination of the neighbourhood and the identification of spatio-temporal dynamical systems is investigated. It is shown that thresholding to convert the pattern to a binary pattern and then applying cellular automata (CA) neighbourhood detection methods can provide an initial estimate of the neighbourhood. A coupled map lattice model can then be identified using the CA detected neighbourhood as the initial conditions. This provides a coarse-to-fine approach for neighbourhood detection and identification of coupled map lattice models. Two examples are used to demonstrate the application of the new approach.

1 Introduction

The modelling, analysis, and control of spatio-temporal dynamical systems present many computational and theoretical challenges with potential applications to physical, chemical, biological, and ecological systems (Kaneko 1993, Sóle, Valls and Bascompte 1992, Yanagita and Kaneko 1997, Tabuchi, Yakawa and Mallick et al 2002, Köhler, Reinhard and Huth 2002). Traditionally such systems have been studied using partial differential equations (PDE's). More recently Coupled Map Lattice (CML) models have emerged as an effective and powerful tool to study these systems due to the computational efficiency and ability to reproduce complex spatio-temporal behaviour. CML models were initiated in the late 80's by Kaneko (1985, 1986, 1989a) and can exhibit surprisingly rich dynamical behaviours, including spatio-temporal chaos, intermittency, traveling waves and pattern formation (Kaneko 1989b). CML's have been used to model convected temperature fluctuations in the atmosphere (Platt and Hammel 1997), boiling processes (Yanagita 1992), spatio-temporal chaos in fluid flows (He, Cao and Li 1995) and cloud dynamics

(Yanagita and Kaneko 1997). Despite the considerable attention devoted to CML's, the identification of CML models from observations or measured data is still regarded as a difficult problem. The aim of this paper is to introduce a new approach to identifying the CML equations from spatio-temporal observations.

Various methods for the identification of local CML models from spatio-temporal observations have already been proposed (Coca and Billings 2001, Billings and Coca 2002, Mandelj, Grabec and Govekar 2001, Marcos-Nikolaus, Martin-Gonzalez and Sóle 2002, Grabec and Mandeji 1997, Parlitz and Merkwirth 2000). An important step in all these modelling methods is the proper reconstruction of the local state vectors at some specified site from the measured data, that is determining the spatio-temporal region which influences the dynamics of that site. This region can be decomposed into two effects: the spatial domain and the time lag. The determination of these two regions is critical for obtaining a good approximation of the underlying spatio-temporal dynamical relationship. In Coca and Billing 2001, and Billings and Coca 2002, the CML equations were restricted to be symmetrically coupled with neighbouring lattice sites within a circular neighbourhood with some finite radius in the spatial domain. In Grabec and Mandeji 1997 and Parlitz and Merkwirth 2000, a state vector was reconstructed from a set of neighbouring values in a rectangular spatio-temporal region while a simple triangular region was used by Mandeji, Garbec and Govekar (2001). Recently, an effective approach to determining the neighbourhood for CA modelling in a binary space has been proposed by Mei and Billings (2002). This motivates our study, and instead of searching for the neighbourhood directly from the original space where real cell entities and CML modelling have to be used, an initial estimate of the neighbourhood is first extracted from an associated binary pattern. The approach involves thresholding the real valued pattern to produce a binary pattern. CA neighbourhood detection methods are then applied to produce an initial neighbourhood to prime the CML modelling. CML identification methods can then be applied to produce the final model. This is a coarse-to-fine modelling strategy which can considerably reduce the computational requirements compared to the more direct approach of searching for the entire neighbourhood in the original space. Providing the main features of the system can be extracted from the thresholded pattern, the approximate neighbourhood should provide a quick method of priming the CML neighbourhood search.

The paper is organised as follows. Section 2 introduces the CML model of spatio-temporal dynamical systems and provides an alternative derivation for the input-output representation. The identification method is presented in section 3 which includes system identification, pattern thresholding and neighbourhood detection. Section 4 illustrates the proposed approach using two examples. Finally conclusions are given in section 5.

2 The CML model

Consider a d-dimensional lattice I consisting of the set of all integer coordinate vectors $i = (i_1, \cdots, i_d) \in \mathbf{Z}^d$. The deterministic CML state-space model of spatio-temporal dynamical systems defined over I is of the following form (Coca and Billings 2001)

$$x_i(t) = f_l(x_i(t-1), u_i(t-1)) + f_c(x_i(t-1), u_i(t-1), \mathbf{s}^m x_i(t-1), \mathbf{s}^m u_i(t-1)) \quad (1)$$

where $x_i(t) \in X_i \subset \mathbf{R}^n$ and $u_i(t) \in U_i \subset \mathbf{R}^l$, X_i and U_i are open sets, n and l-dimensional vectors representing the local state and input variables respectively at the ith site in I, and f_l and f_c are piecewise differentiable maps. $\mathbf{s}^m$ is a spatial shift operator, which is defined as

$$\mathbf{s}^m = (s^{p_1}, s^{p_2}, \cdots, s^{p_m}) \quad (2)$$

such that

$$\mathbf{s}^m x_i(t) = (s^{p_1} x_i(t), s^{p_2} x_i(t), \cdots, s^{p_m} x_i(t)) = (x_{i+p_1}(t), x_{i+p_2}(t), \cdots, x_{i+p_m}(t)) \quad (3)$$

where $p_1, p_2, \cdots, p_m$ are the indices of the neighbours of the ith site - that is the region in I around the ith site, which influences the dynamics of that site.

The CML model (1) can also be written, in terms of the global state and input variables $x = \{x_i\}_{i \in I} \subset X = \prod_{i \in I} X_i$ and $u = \{u_i\}_{i \in I} \subset U = \prod_{i \in I} U_i$, as follows

$$x(t) = f(x(t-1), u(t-1)) \quad (4)$$

where $f : X \times U \to X$ is the function sequence $f = \{f_i\}_{i \in I}$ with $f_i = f_l + f_c$ and $i = \{i_1, \cdots, i_d\} \in I$.

In general, the direct measurement of the state vector x is not possible and only some observable variable y which depends on the state and input can be measured. Therefore, the state-space model of the CML is usually complemented with a measurement equation

$$y_i(t) = h_i(x(t)) \quad (5)$$

Here it is assumed that the measurement function is identical for each site, i.e., $h_i = h$. Furthermore, it is assumed that the lattice equations are spatially invariant over the observed spatial domain. This implies that the difference equations corresponding to each lattice site or location are the same for all lattice sites. Generally it is also assumed that the following input-output representation

$$y_i(t) = g(\mathbf{q}^{n_y} y_i(t), \mathbf{q}^{n_u} u_i(t), \mathbf{s}^{m'} \mathbf{q}^{n_y} y_i(t), \mathbf{s}^{m'} \mathbf{q}^{n_u} u_i(t)) \quad (6)$$

can be derived for any site from (1) and (5). In (6), $\mathbf{q}$ is a backward shift operator such that

$$\mathbf{q}^{n_y} y_i(t) = (y_i(t-1), y_i(t-2), \cdots, y_i(t-n_y)) \quad (7)$$

A number of sufficient conditions which ensure that this can be found are given in Billings and Coca 2002 for the symmetric or anti-symmetric coupling cases Here an alternative derivation of this result for a more general case is given below.

From the measurement equation (5) and state equation (1),

$$\begin{aligned} y_i(t) &= h_i(x(t)) =: \Phi_i^1(x(t)) \\ y_i(t+1) &= h_i(x(t+1)) = h_i \circ f(x(t), u(t)) =: \Phi_i^2(x(t), u(t)) \\ &\vdots \\ y_i(t+n_y-1) &= h_i(x(t+n_y-1)) = h_i \circ f^{n_y-1}(x(t), u(t)) \\ &=: \Phi_i^{n_y}(x(t), u(t), u(t+1), \cdots, u(t+n_y-2)) \end{aligned}$$

where $\circ$ denotes the composition of functions. Then

$$\begin{aligned} \mathbf{s}^m y_i(t) &= \mathbf{s}^m h_i(x(t)) = \mathbf{s}^m \Phi_i^1(x(t)) \\ \mathbf{s}^m y_i(t+1) &= \mathbf{s}^m h_i(x(t+1)) = \mathbf{s}^m \Phi_i^2(x(t), u(t)) \\ &\vdots \\ \mathbf{s}^m y_i(t+n_y-1) &= \mathbf{s}^m h_i(x(t+n_y-1)) = \mathbf{s}^m \Phi_i^{n_y}(x(t), u(t), u(t+1), \cdots, u(t+n_y-2)) \end{aligned}$$

Let $Y_i(t) = (y_i(t), y_i(t+1), \cdots, y_i(t+n_y-1), \mathbf{s}^m y_i(t), \mathbf{s}^m y_i(t+1), \cdots, \mathbf{s}^m y_i(t+n-1))^T$, $U(t) = (u(t), u(t+1), \cdots, u(t+n_y-2))^T$, and $\Phi_i = (\Phi_i^1, \Phi_i^2, \cdots, \Phi_i^n, \mathbf{s}^m\Phi_i^1, \mathbf{s}^m\Phi_i^2, \cdots, \mathbf{s}^m\Phi_i^{n_y})^T$, then it follows that

$$Y_i(t) = \Phi_i(x(t), U(t)) \tag{8}$$

If Φ_i is a C^r map (differentiable up to r), $r \geq 1$ and the partial derivatives of Φ_i in the measurement site i with respect to $x(t)$ are isomorphic with respect to $U(t)$, then from the implicit function theorem in Banach space that $x(t)$ can be expressed locally in terms of $Y_i(t)$ and $U(t)$ which implies

$$y_i(t+n_y) = h_i(x(t+n_y)) = \Phi_i^{n_y+1}(x(t), u(t), u(t+1), \cdots, u(t+n_y-1)) \tag{9}$$

that is

$$\begin{aligned} y_i(t) &= g'(y_i(t-1), y_i(t-2), \cdots, y_i(t-n_y); \\ &\quad \mathbf{s}^m y_i(t-1), \mathbf{s}^m y_i(t-2), \cdots, \mathbf{s}^m y_i(t-n_y); u(t-1), u(t-2), \cdots, u(t-n_y)) \\ &= g'(\mathbf{q}^{n_y} y_i(t), \mathbf{s}^m \mathbf{q}^{n_y} y_i(t), \mathbf{q}^{n_y} u(t)) \end{aligned} \tag{10}$$

In practice, it is reasonable to expect that the measurement function $y_i(t)$ will depend only on a finite number of states and input variables in the neighbourhood of the measurement site, then (10) can be rewritten in the following form

$$y_i(t) = g(\mathbf{q}^{n_y} y_i(t), \mathbf{q}^{n_u} u_i(t), \mathbf{s}^{m'} \mathbf{q}^{n_y} y_i(t), \mathbf{s}^{m'} \mathbf{q}^{n_u} u_i(t)) \tag{11}$$

3 CML identification

3.1 The identification procedure

From (11), the task of the identification is to reproduce the dynamical relation g from the measured data. For a specific site i, the identification procedure can be outlined as below

i) Determine the spatial neighbourhood sites (represented by $\mathbf{s}^{m'}$) of the ith site;

ii) Determine the time lags n_y and n_u;

iii) Apply the Orthogonal Least Squares (OLS) algorithm to obtain the parameters of the CML model (polynomials as regressors).

If data is available from more sensors than the minimum required to extract the CML equations, the additional measurements can be used in model validation. The CML model identified using a set of data from a given spatial site can be validated on data recorded at different spatial locations by computing the model predicted output

$$\hat{y}_j(t) = \tilde{g}(\mathbf{q}^{n_y} \hat{y}_j(t), \mathbf{q}^{n_u} u_j(t), \mathbf{s}^{m'} \mathbf{q}^{n_y} \hat{y}_j(t), \mathbf{s}^{m'} \mathbf{q}^{n_u} u_j(t)) \tag{12}$$

Model predicted output is a much more rigorous test than one step ahead predicted outputs which most authors use.

Note that in the above identification procedure, the spatial neighbourhood sites (represented by $\mathbf{s}^{m'}$) of the identified site and the time lags (n_y, n_u) need to be known *a priori*. In other words, the neighbourhood of the identified site, i.e., the region around that site which influences the dynamics of that site in the spatial domain and the time domain need to be known before starting the identification. In practice, these two factors are important in determining the spatio-temporal dynamics of the underlying system. Determining which site and what time lag should be included in the model structure is therefore very important in CML identification. Whilst Chen and Billings (1990) proposed an algorithm for time lag determination which has been used in many applications, little progress has been made in the determination of the spatial neighbourhood. As noted in section 1, existing methods tend to choose a circular, rectangular or triangular region around the identified site as the initial spatial neighbourhood. In the following

sections, a novel approach will be presented to detect the initial neighbourhood using thresholding and a CA method.

3.2 Feature extraction by thresholding

In this study, thresholding will be applied to extract the main features of a spatio-temporal dynamical system. For a real-value spatio-temporal dynamical system, snapshots of the evolution of the system both in time and space show up as a series of images which represent the features of the underlying dynamical system. The features in these images are reflected by the magnitude distribution of the variables, generally real entities, over a spatial domain of interest at some specific time instants. By thresholding these images to form binary counterparts, the main features of the original system may, depending on the dynamics of the patterns involved, be retained using only two-levels, which significantly reduces the computational requirements for searching for candidate neighbours.

The thresholding process can be accomplished using histograms. The basic procedure is as follows

i) Produce a histogram of the measured or simulated data from the underlying spatio-temporal system;

ii) Determine the threshold value by setting it as some value between the peaks or the centre of the distribution occurring in the histogram;

iii) Generate a binary spatio-temporal data set.

3.3 Initial Neighbourhood detection using CA's

The feature extraction process above produces an approximate binary representation of the spatio-temporal pattern. Applying this procedure to the input-output measurements $(u_i(t), y_i(t))$ of the underlying spatio-temporal system, therefore produces a collection of corresponding binary data $(u_i^*(t), y_i^*(t))$. The assumption is that a dynamical relationship exists among these binary input-output data which partially represents the main features of the original dynamical system (6). Assume that the spatio-temporal dynamical relationship (6) can be expressed by a CA model counterpart in binary space

$$y_i^*(t) = g(\mathbf{q}^{n_y} y_i^*(t), \mathbf{q}^{n_u} u_i^*(t), \mathbf{s}^{m'} \mathbf{q}^{n_y} y_i^*(t), \mathbf{s}^{m'} \mathbf{q}^{n_u} u_i^*(t)) \tag{13}$$

The approach developed by Mei and Billings (2002) can then be employed to detect the neighbourhood both in the spatial domain and the time domain for the thresholded data $(u_i^*(t), y_i^*(t))$. Initially, assume the CA model has the following structure

$$y_i^*(t) = g(\mathbf{q}^{n_{y0}} y_i^*(t), \mathbf{q}^{n_{u0}} u_i^*(t), \mathbf{s}^{m'0} \mathbf{q}^{n_{y0}} y_i^*(t), \mathbf{s}^{m'0} \mathbf{q}^{n_{u0}} u_i^*(t)) \tag{14}$$

where n_{y0}, n_{u0}, and m'_0 are the candidate time lags and the spatial range. The candidate term vector is therefore

$$(\mathbf{q}^{n_{y0}} y_i^*(t), \mathbf{q}^{n_{u0}} u_i^*(t), \mathbf{s}^{m'_0}\mathbf{q}^{n_{y0}} y_i^*(t), \mathbf{s}^{m'_0}\mathbf{q}^{n_{u0}} u_i^*(t)) \in B^{(m'_0+1)\times(n_{y0}+n_{u0})}$$

$B = \{0, 1\}$, and the result from Mei and Billings (2002) can be used to determine the neighbourhood for (13) if the candidate set is large enough:

Proposition 1 Let $y = f(x_1, x_2, \cdots, x_n)$ be a Boolean function from B^n to B, $B = \{0, 1\}$. For any given component x_i, there exists a Boolean function $f' : B^{n-1} \to B$, $f'(x_1, \cdots, x_{i-1}, x_{i+1}, \cdots, x_n) \in B$ such that $f = f' \circ p_i$, where p_i is the natural projection from B^n to the other $n-1$ components except i if and only if

$$f(x_1, \cdots, x_{i-1}, 1 - x_i, x_{i+1}, \cdots, x_n) \equiv f(x_1, \cdots, x_{i-1}, x_i, x_{i+1}, \cdots, x_n) \tag{15}$$

for all $[x_1, \cdots, x_{i-1}, x_{i+1}, \cdots, x_n] \in B^{n-1}$.

Condition (15) implies that the ith component makes no contribution to the Boolean function f so that it can be discarded. Repeatly applying the above proposition to (14), produces a minimal collection of components which represent the neighbourhood. This neighbourhood can then be used to prime the CML identification.

Obviously this strategy will work well when the dynamics of the CML pattern, can be reasonably approximated by a binary pattern. There will be cases where this is not the case. However, our simulations suggest that this approach works well in many examples. The advantage is that the neighbourhood search over the binary pattern is very straightforward and relatively quick. This is then used to prime CML identification and can be considered as a coarse-to-fine approach to neighbourhood detection. The histogram of the original pattern provides a good indicator of whether the method will work well and this can be used as the decision boundary. Little computing effort will have been wasted even if the histgram suggests the method may not be appropriate for a particular spatio-temporal pattern. If the coarse-to-fine neighbourhood detection method is however applied model validation, based for example on the CML model predicted output, should be used as a means of testing the authenticity of the final CML model.

4 Simulation studies

4.1 Example 1 - Linear Diffusion Equation

Consider the following diffusion equation

$$\frac{\partial^2 v(t,x)}{\partial t^2} - C\frac{\partial^2 v(t,x)}{\partial x^2} = u(t,x), x \in [0,1] \tag{16}$$

with initial conditions

$$\begin{aligned} v(0,x) &= 0 \\ \frac{dv(0,x)}{dt} &= 4\exp(-x) + \exp(-0.5x) \end{aligned} \tag{17}$$

where

$$u(t,x) = -13\exp(-x)\cos(1.5t) - 9.32\exp(-0.5x)\cos(2.1t) \tag{18}$$

For $C = 1.0$ the exact solution $v(t,x)$ of the initial value problem (16), (18) is

$$\begin{aligned} v(t,x) &= 4\exp(-x)\cos(1.5t) + 2\exp(-0.5x)\cos(2.1t) \\ &\quad -4\exp(-x)\exp(-t) - 2\exp(-0.5x)\exp(-0.5t) \end{aligned} \tag{19}$$

The measurement function was taken as

$$y(t,x) = v(t,x) \tag{20}$$

The reference solution was sampled at 21 equally spaced points over the spatial domain $\Omega = [0,1], x = \{x_1, \cdots, x_{21}\} = (0, 0.05, \cdots, 0.95, 1)$. From each location, 1000 input/output data points sampled at $\Delta t = \pi/100$ were generated. The data are plotted in Fig.(1).

The histogram of the input/output data is shown in Fig.(2) which exhibits a normal-like distribution. Therefore, the threshold value was set to be zero to obtain a binary counterpart of the original pattern. The corresponding binary pattern is shown in Fig.(3). The obtained neighbourhood from cellular automata was $i-1, i+1$, and $i+2$ in the spatial domain and $t-1, t-2$ in the time domain. This estimated neighbourhood comprises the neighbourhood, $i-1$ and $i+1$, used in Billings and Coca 2002, which indicates the rationale for using the proposed strategy. Using the neighbourhood as an initial estimation, different combinations of the sites within this were tested for the CML modelling. The case, which the neighbourhood was selected to be $i-1$ and $i+1$ in the spatial domain and $t-1, t-2$ in the time domain without the symmetrical restrictions, is presented here.

The identification data consisted of 1000 data points of input/output data $u_i(t), y_i(t)$ at site $i = 3$ corresponding to $x = x_3 = 0.1$. In addition, 1000 input and output data $u_i(t), y_{i-1}(t)$ and $y_{i+1}(t)$ from neighbouring locations $x = x_2 = 0.05$ and $x = x_4 = 0.15$ acted as inputs during the identification. The identified model is listed in Table (1), where ERR denotes the Error Reduction Ratio (Chen and Billings 1989) and STD denotes the standard deviations. It is shown

Terms	Estimates	ERR	STD
$y_i(t-1)$	0.16799E+01	0.99734E+00	0.11860E+00
$y_i(t-2)$	-0.99911E+00	0.26578E-02	0.86569E-11
$u_i(t-1)$	0.97171E-03	0.16440E-05	0.14638E-12
$y_{i-1}(t-1)$	0.16906E+00	0.89148E-07	0.57112E-01
$y_{i+1}(t-1)$	0.15065E+00	0.83493E-15	0.61560E-01
constant	0.78551E-17	0.41257E-16	0.42323E-15
$u_i(t-2)$	0.14685E-04	0.24471E-17	0.14312E-12
$y_{i-1}(t-2)$	-0.79775E-03	0.35227E-15	0.77924E-11

Table 1: Example 1: The terms and parameters of the final CML model

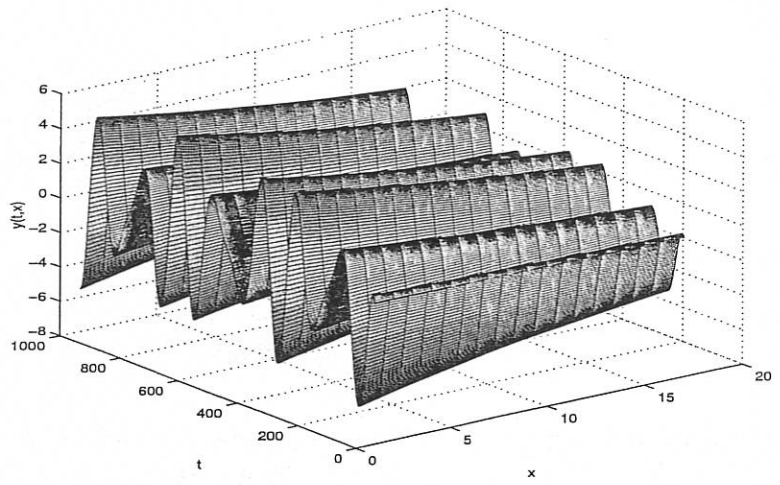

Figure 1: Example 1: System output

that the number of terms in the identified model is 8 which is less then that (9 terms) from Billing and Coca 2002.

The model predicted output is plotted in Fig.(4), which shows very good agreement between the exact solution and the CML model output.

4.2 Example 2 - Sine-Gordon Equation

Consider the two-dimensional Sine-Gordon Equation (Hirota 1973)

$$\frac{\partial^2 u(t,x,y)}{\partial x^2} + \frac{\partial^2 u(t,x,y)}{\partial y^2} - \frac{\partial^2 u(t,x,y)}{\partial t^2} = \sin(u(t,x,y)) \tag{21}$$

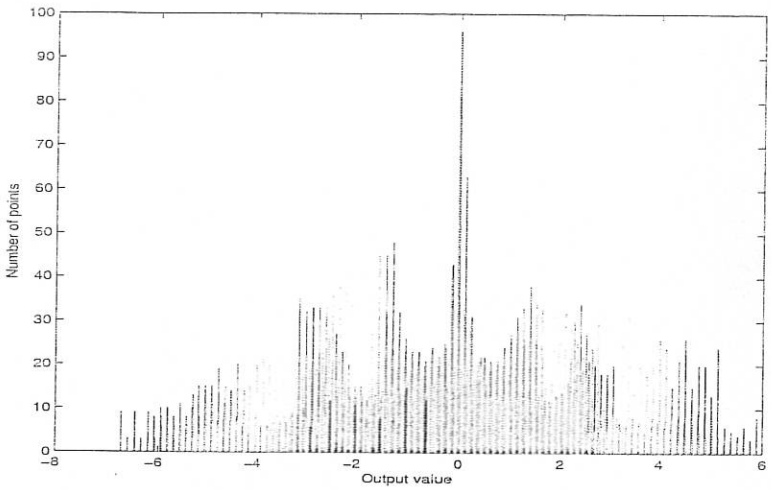

Figure 2: Example 1: Histogram of the data

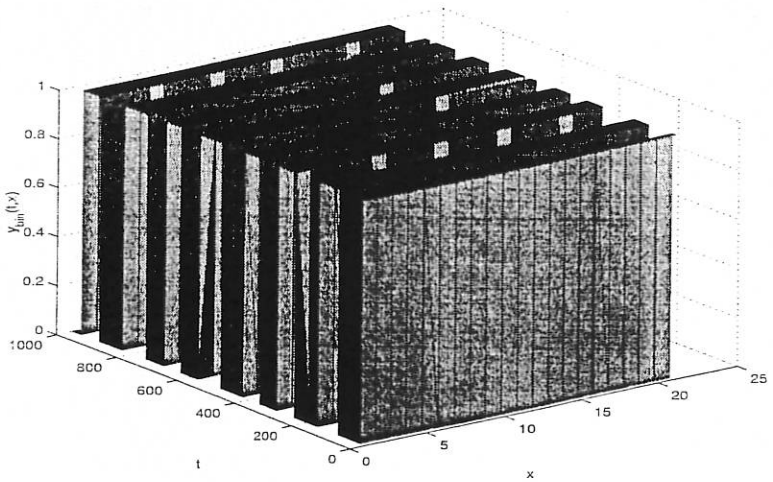

Figure 3: Example 1: Binary output

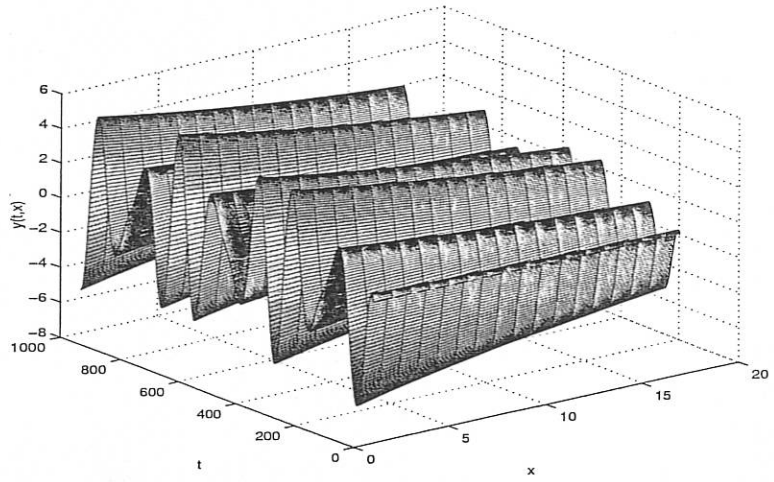

Figure 4: Example 1: Model predicted output

which describes the motion of the magnetic flux quanta on a Josephson junction transmission line.

The exact three-soliton solution of (21) can be expressed in the following form

$$u(t,x,y) = 4\tan^{-1}(\frac{g(t,x,y)}{f(t,x,y)}) \tag{22}$$

where

$$\begin{aligned} f(t,x,y) &= 1 + a(1,2)\exp(\eta_1+\eta_2) + a(1,3)\exp(\eta_1+\eta_3) + a(2,3)\exp(\eta_2+\eta_3) \\ g(t,x,y) &= \exp(\eta_1) + \exp(\eta_2) + \exp(\eta_3) + a(1,2)a(1,3)a(2,3)\exp(\eta_1+\eta_2+\eta_3)) \end{aligned} \tag{23}$$

in which

$$\begin{aligned} a(i,j) &= \frac{(P_i-P_j)^2 + (q_i-q_j)^2 - (w_i-w_j)^2}{(P_i+P_j)^2 + (q_i+q_j)^2 - (w_i+w_j)^2} \\ \eta_i &= P_i x + q_i y - w_i t - \eta_i^0, (\eta_i^0 \text{ is constant}) \\ P_i^2 + q_i^2 - w_i^2 &= 1, \text{for } i,j = 1,2,3 \end{aligned}$$

provided that the parameters P_i, q_i, and $w_i, i = 1,2,3$ satisfy the condition

$$det\begin{pmatrix} P_1 & q_1 & w_1 \\ P_2 & q_2 & w_2 \\ P_3 & q_3 & w_3 \end{pmatrix} = 0$$

The solution (22) was sampled at 50×50 spaced points with $\Delta h = 0.05$ with the following parameter values, $P_1 = 1.1, P_2 = P_3 = 0.3; q_1 = 0.0, q_2 = q_3 = 1.2$ and $w_1 = 0.4583, w_2 = w_3 = 0.6633$, and initial conditions

$$u(0, x, y) = 4\tan^{-1}(\frac{g(0, x, y)}{f(0, x, y)}) \tag{24}$$

The measurement function was taken as

$$y(t, x, y) = u(t, x, y) \tag{25}$$

From each location, 100 input/output data points sampled at $\Delta t = 0.1$ were generated. Fig.(5) shows four snapshots of $y(t, x, y)$ at $t = 0, t = 0.1 \times 10 = 1, t = 0.1 \times 20 = 2$ and $t = 0.1 \times 30 = 3$, respectively. Fig.(6) shows the time series of the system outputs.

The histogram of all input/output data is shown in Fig.(7) which clearly exhibits two peaks which suggests a suitable threshold value would lie between these two peaks. The threshold value was therefore set to be 2 in this simulation. The obtained neighbourhood from cellular automata was $(i-1, j), (i-1, j-1), (i, j-2), (i-2, j)$, and $(i, j-3)$ in the spatial domain and $t-1$ in the time domain.

The identification data consisted of 30 data points of input/output data $u_i(t), y_i(t)$ at the node $(i, j) = (25, 25)$. The identified model is listed in Table (2)

The model predicted outputs are plotted in Fig.(8), which show that the identified CML model can reproduce the spatio-temporal patterns of the original system very well.

5 Conclusions

A novel approach to the identification of spatio-temporal dynamical systems has been introduced. It has been demonstrated that determining the neighbourhood for a real-value CML model can be significantly simplified by employing a binary counterpart of the original data. Computing a histogram of the data provides a good indication of whether this coarse-to-fine neighbourhood detection algorithm will be worthwhile. Simulation results were included to demonstrate that the coarse-to-fine procedure can produce excellent final CML models with a significant reduction in computational resource.

6 Acknowledgement

The authors gratefully acknowledge financial support from EPSRC (UK).

Terms	Estimates	ERR	STD
$y_{i,j-2}(t-1)$	0.85718E+00	0.99999E+00	0.11960E+01
$y_{i-2,j}(t-1)$	0.38689E+00	0.11733E-05	0.52748E+00
$y_{i,j-3}(t-1)$	-0.27956E+00	0.28690E-07	0.81747E+00
constant	-0.14333E-04	0.10377E-10	0.25698E-04
$y_{i-1,j}(t-1)$	0.60874E-01	0.47631E-11	0.10475E+01
$y^2_{i-2,j}(t-1)$	-0.14189E-01	0.11647E-13	0.11793E+00
$y_{i,j}(t-1)$	-0.26475E-01	0.16857E-14	0.23102E+00
$y^2_{i-1,j}(t-1)y_{i-1,j-1}(t-1)$	0.87364E-02	0.10906E-15	0.37293E-01
$y_{i,j}(t-1)y_{i-1,j-1}(t-1)y_{i-2,j}(t-1)$	0.39445E-01	0.14168E-14	0.10067E+00
$y_{i-1,j-1}(t-1)y_{i,j-2}(t-1)$	0.65649E-01	0.91298E-14	0.49675E+00
$y^2_{i,j-2}(t-1)$	-0.49985E-01	0.72695E-14	0.37229E+00
$y_{i-1,j}(t-1)y_{i-1,j-1}(t-1)$	-0.12208E-02	0.12146E-13	0.13893E-01
$y_{i-1,j}(t-1)y^2_{i-2,j}(t-1)$	0.78280E-03	0.10020E-13	0.26307E-01
$y_{i,j}(t-1)y_{i-2,j}(t-1)y_{i,j-3}(t-1)$	0.24243E-01	0.53862E-14	0.77486E-01
$y_{i-1,j}(t-1)y_{i,j-2}(t-1)y_{i,j-3}(t-1)$	0.18671E-02	0.45060E-14	0.16395E-01
$y_{i,j}(t-1)y_{i-1,j}(t-1)y_{i,j-2}(t-1)$	0.21671E-01	0.29832E-14	0.40881E-01
$y_{i-1,j}(t-1)y_{i-2,j}(t-1)y_{i,j-3}(t-1)$	-0.10455E-01	0.12683E-14	0.11613E-01
$y_{i,j}(t-1)y_{i,j-2}(t-1)y_{i-2,j}(t-1)$	-0.66183E-01	0.12633E-14	0.14130E+00
$y_{i,j-2}(t-1)y^2_{i,j-3}(t-1)$	-0.13504E-02	0.12183E-14	0.10186E-01
$y_{i,j}(t-1)y_{i-1,j}(t-1)y_{i-2,j}(t-1)$	-0.18752E-01	0.11756E-14	0.42723E-01

Table 2: Example 2: The terms and parameters of the final CML model

References

[1] Billings, S. A. and Coca, D., (2002) Identification of coupled map lattice models of deterministic distributed parameter systems, *Int. J. Syst. Sci.*, In Print.

[2] Chen, S. and Billings, S. A., (1989) Modelling and analysis of non-linear time series. *International Journal of Control*, Vol. 50, No. 6, pp. 2151-2171.

[3] Coca,D. and Billings, S. A., (2001) Identification of coupled map lattice models of complex spatio-temporal pattern, *Phys. Lett.*, A287, pp. 65-73.

[4] Grabec, I. and Mandelj, S., (1997) Continuation of chaotic fields By RBFNN, in *Biological and Artificial Computation: From Neuroscience to Technology: Proc.*, Mira, J. et al. eds., Lecture Notes in Computer Science, Springer-Verlag, Vol. 1240, pp. 597-606.

[5] He, G., Cao, L., and Li, J., (1995) Convective coupled map for simulating spatiotemporal chaos in flows, *Acta Mechanica Sinica*, Vol. 11, pp. 1-7.

[6] Hirota, R., (1973) Exact three-soliton of the two-dimensional Sine-Gordon equation, *J. Phys. Soc. Japan*, Vol. 35, pp. 1566.

[7] Kaneko, K., (1985) Spatio-temporal intermittency in couple map lattices, *Progress of Theoretical Physics*, Vol. 74, No. 5, pp. 1033-1044.

[8] Kaneko, K., (1986) Tuebulence in coupled map lattices, *Physica*, D18, pp. 475-476.

[9] Kaneko, K., (1989a) Spatiotemporal chaos in one- and two-dimensional coupled map lattices, *Physica*, D37, pp. 60-82.

[10] Kaneko, K., (1989b) Pattern dynamics in spatiotemporal chaos: pattern selection, diffusion of defect and pattern competition intermittency, *Physica*, D34, pp. 1-41.

[11] Kaneko, K. (eds.), (1993) *Coupled map lattice: theory and experiment*, World Scientific, Singapore.

[12] Köhler, P., Reinhard, K., and Huth, A., (2002) Simulating anthropogenic impacts to bird communities in tropical rain forests, *Biological Conservation*, Vol. 108, pp. 35-47.

[13] Mandelj, S., Grabec, I., and Govekar, E, (2001) Statistical approach to modeling of spatiotemporal dynamics, *Int. J. Bifurcation & Chaos*, Vol. 11, No. 11, pp. 2731-2738.

[14] Marcos-Nikolaus, P., Martin-Gonzalez, J. M. and Sóle, R. V., (2002) Spatial forcasting: detecting determinism from single snapshots, *Int. J. Bifurcation and Chaos*, Vol. 12, No. 2, pp. 369-376.

[15] Mei, S. S. and Billings, S. A., (2002) Neighbourhood determination and transition rule identification for deterministic cellular automata, *Research Report of The University of Sheffield, UK.*

[16] Parlitz, U. and Merkwirth, C., (2000) Prediction of spatiotemporal teim series based on reconstructed local states, *Phys. Rev. Lett.* , Vol. 84, No. 9, pp. 2820-2823.

[17] Platt, N. and Hammel, S., (1997) Pattern formation in driven coupled map lattices, *Physica*, A239, No. 1-3, pp. 296-303.

[18] Sóle, R. V., Valls, J. and Bascompte, J., (1992) Spiral waves, chaos and multiple attactors in lattice models of interacting populations, *Phys. Lett.*, A166, No. 2, pp. 123.

[19] Tabuchi, E., Yakawa, T., Mallick, H., Inubushi, T., Kondoh, T., Ono, T., and Torii, K., (2002) Spatio-temporal dynamics of brain activated regions during drinking behaviour in rats, *Brain Research*, Vol. 951, pp. 270-279.

[20] Yanagita, T., (1992) Phenomenology of boiling: a coupled map lattice model, *Chaos*, Vol. 2, No. 3, pp. 343-350.

[21] Yanagita, T. and Kaneko, K, (1997) Modeling and characterisation of cloud dynamics, *Phys. Rev. Lett.*, Vol. 78, No. 22, pp. 4297-4300.

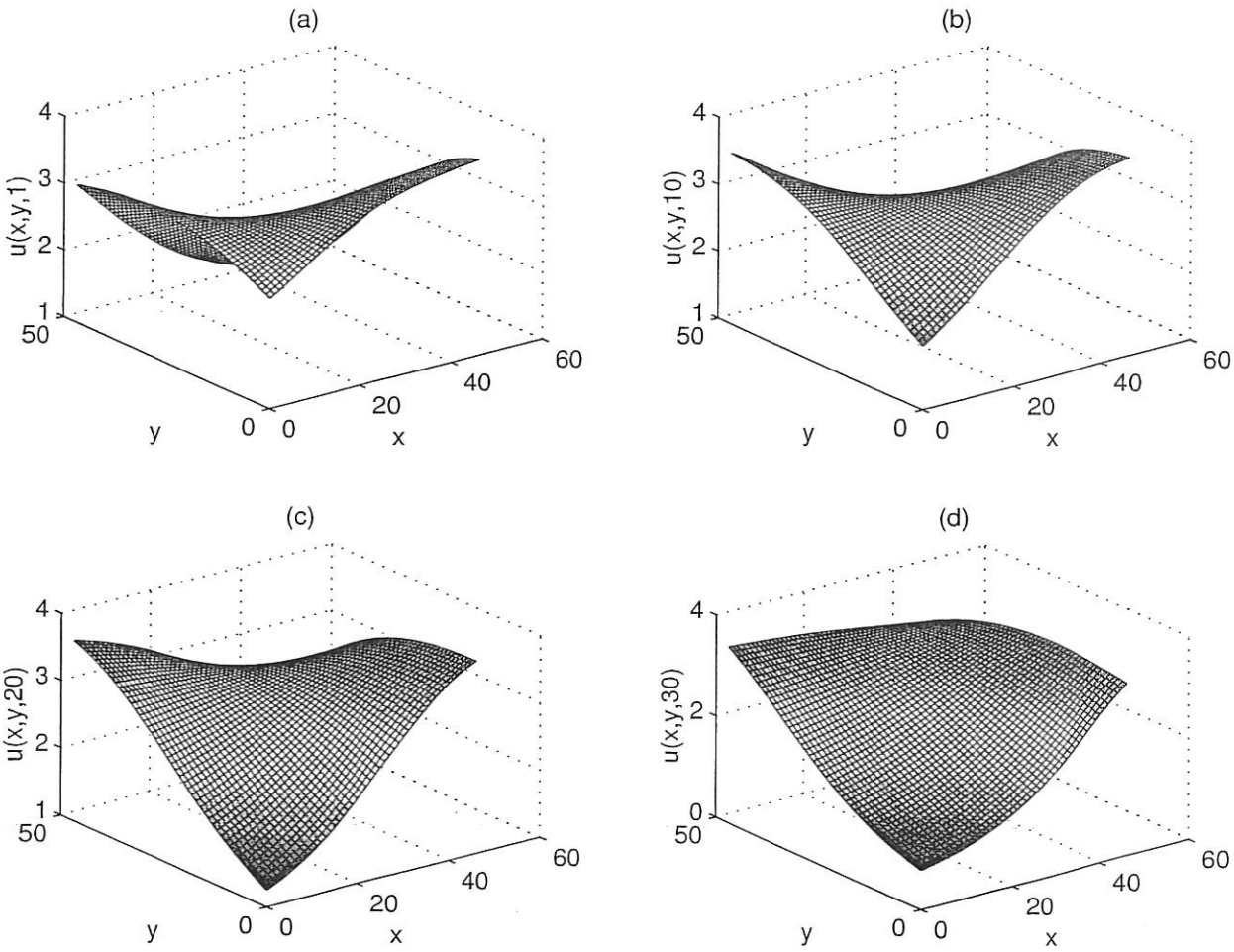

Figure 5: Example 2: Sytem outputs at (a) $t = 0$, (b) $t = 0.1 \times 10 = 1$, (c) $t = 0.1 \times 20 = 2$, (d) $t = 0.1 \times 30 = 3$

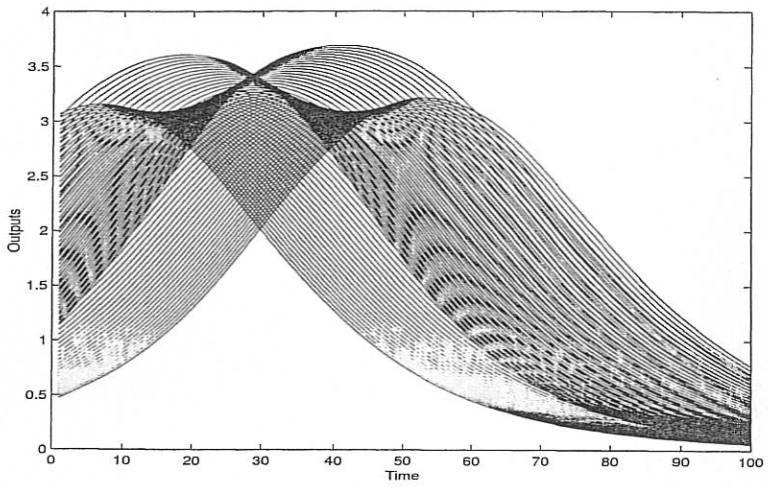

Figure 6: Example 2: Time series of the system output

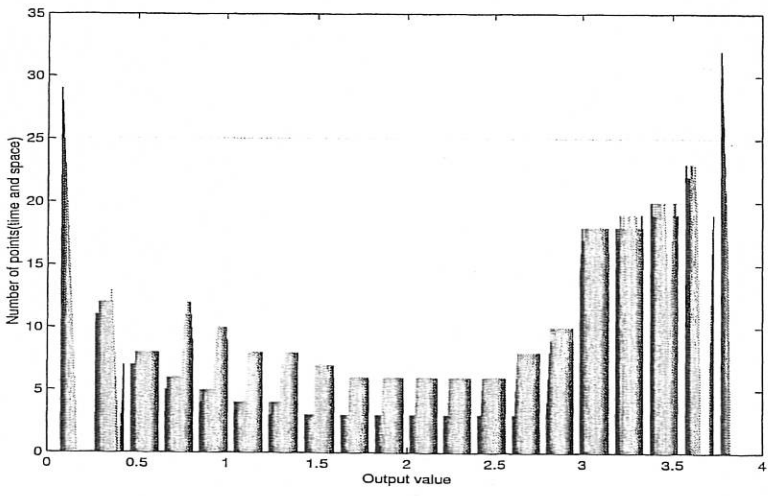

Figure 7: Example 2: Histogram of the data

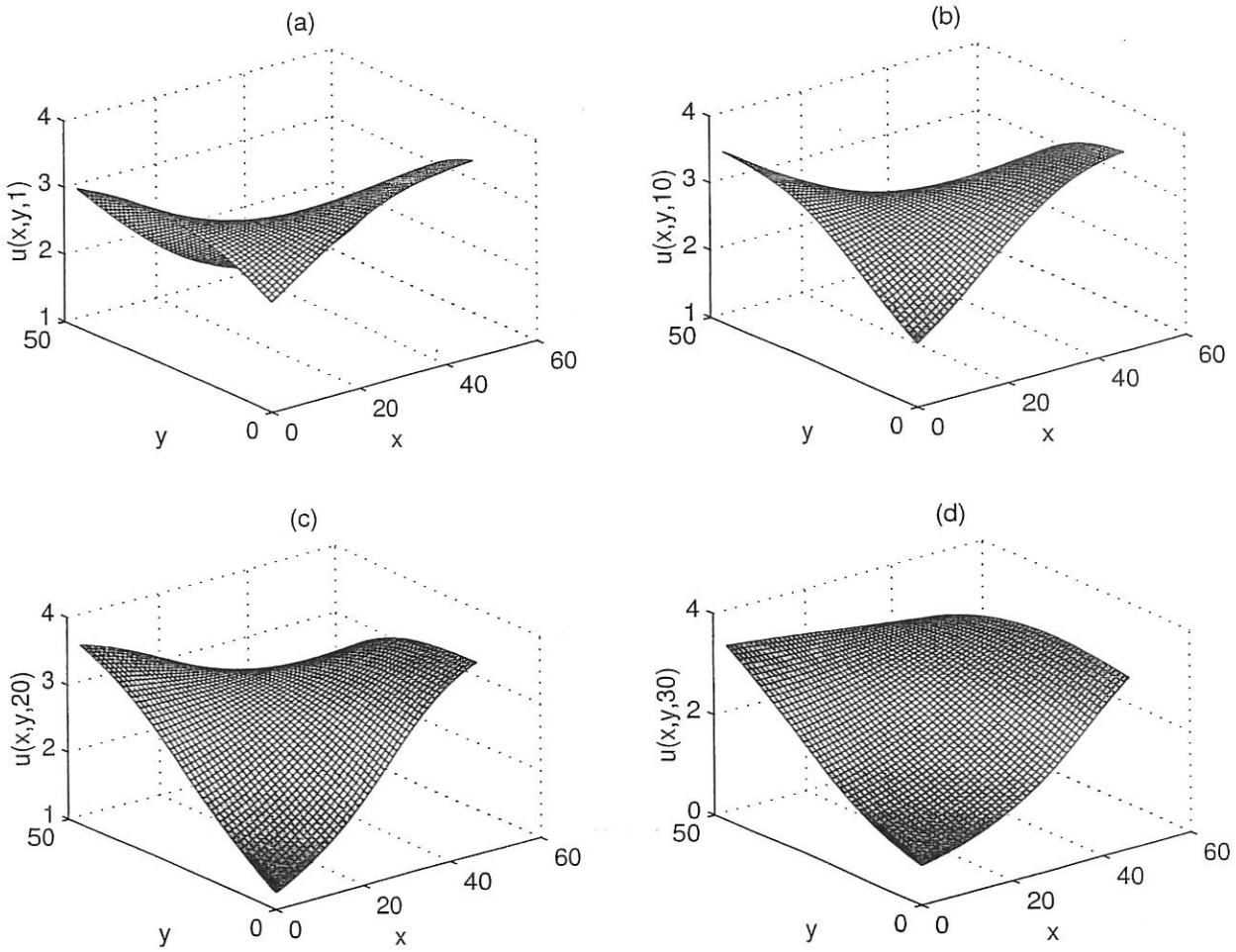

Figure 8: Example 2: Model predicted output at (a) $t = 0$, (b) $t = 0.1 \times 10 = 1$, (c) $t = 0.1 \times 20 = 2$, (d) $t = 0.1 \times 30 = 3$